RESEARCH PAPER

Quality-by-Design Optimisation of PLGA and Eudragit RS100 Nanoparticles for Combined Oral Delivery of Glimepiride and Empagliflozin: A Box–Behnken Approach

Dr. Rahul S. Solunke[1*], Rutuja Pimple[2]

[1]Godavari Institute of Pharmacy, Kolpa, Latur - Nanded Highway, Latur 413512, Email: solunkerahul1986@gmail.com, Orcid id : 0000-0002-6915-517X*

[2]M. Pharmacy Scholar Godavari institute of pharmacy kolpa

Corresponding Author

Dr. Rahul S. Solunke

Godavari Institute of Pharmacy, Kolpa, Latur - Nanded Highway, Latur 413512, Email: solunkerahul1986@gmail.com, Orcid id : 0000-0002-6915-517X

ABSTRACT

Background: Glimepiride (GLM) and empagliflozin (EMP) are mechanistically complementary BCS Class II antidiabetic agents whose oral bioavailability is limited by poor aqueous solubility and dissolution-rate-limited absorption. No polymeric nanoparticulate platform for the combined delivery of these two agents has previously been reported. Methods: GLM-loaded poly(lactic-co-glycolic acid) (PLGA) nanoparticles were prepared by nanoprecipitation and EMP-loaded Eudragit RS100 nanoparticles by emulsification-solvent evaporation. Critical formulation variables (PLGA/Eudragit concentration, drug:polymer ratio, and polyvinyl alcohol concentration) were optimised using a Quality-by-Design (QbD), Box–Behnken response-surface design after risk assessment of formulation, process, stabiliser and material variables. UV-spectrophotometric quantification was validated per ICH Q2(R1); accelerated stability followed ICH Q1A(R2). Results: The fitted quadratic models explained 97.2%, 99.6% and 97.2% of the variance in particle size, entrapment efficiency and polydispersity index, respectively (overall model F up to 198.7). The optimised GLM-PLGA and EMP-Eudragit RS100 nanoparticles measured 172.6 ± 4.2 nm and 184.3 ± 5.6 nm, with entrapment efficiencies of 84.2 ± 1.8% and 81.6 ± 2.1%. Cumulative 24-hour release reached 94.2 ± 3.2% (GLM-NPs) and 91.6 ± 2.9% (EMP-NPs), a 3.3- and 3.5-fold enhancement over the respective pure-drug suspensions, best described by the Korsmeyer–Peppas model (R^2 = 0.992 and 0.991; n ≈ 0.52, anomalous transport). Both formulations remained within ICH-acceptable limits after 3 months of storage at 40 °C/75% RH. Conclusion: A Box–Behnken-optimised dual-polymer nanoparticulate platform markedly enhances the in vitro dissolution of both GLM and EMP, providing a scientifically justified, regulatory-aligned foundation for further in vivo bioavailability evaluation in Type 2 Diabetes Mellitus.

Keywords: Glimepiride; Empagliflozin; PLGA nanoparticles; Eudragit RS100; Box–Behnken design; Quality by Design; Type 2 diabetes mellitus; oral bioavailability

How to cite this article: Rahul S. Solunke1* Rutuja Pimple2. Quality-by-Design Optimisation of PLGA and Eudragit RS100 Nanoparticles for Combined Oral Delivery of Glimepiride and Empagliflozin: A Box–Behnken Approach. Int J Drug Deliv Technol. 2026;16(80s):1153-1155. DOI: 10.25258/ijddt.16.80s.144.

INTRODUCTION

The oral route remains the most widely used and best-tolerated mode of systemic drug delivery, yet its clinical performance for many agents is constrained by poor aqueous solubility, dissolution-rate-limited absorption, and extensive hepatic first-pass metabolism [1,2]. Approximately 40% of marketed drugs and nearly 90% of new chemical entities in development exhibit poor aqueous solubility [2]. The Biopharmaceutics Classification System (BCS) places such high-permeability, low-solubility compounds in Class II, where oral absorption is rate-limited by dissolution rather than membrane permeation [1]. Glimepiride (GLM), a third-generation sulfonylurea insulin secretagogue, and empagliflozin (EMP), a selective sodium-glucose cotransporter-2 (SGLT-2) inhibitor, are both BCS Class II antidiabetic agents whose aqueous solubility (< 0.004 mg/mL and < 0.1 mg/mL, respectively, at pH 7.4) restricts dissolution and produces variable oral bioavailability [8,9].

Polymeric nanoparticles (PNPs) - sub-micron colloidal carriers fabricated from biodegradable polymers such as poly(lactic-co-glycolic acid) (PLGA), Eudragit RS/RL100, polycaprolactone, and chitosan - are among the most extensively investigated platforms for overcoming the dissolution limitations of BCS Class II drugs [4,6]. The nanometric size dramatically increases the surface area available for dissolution, can promote transcytosis and M-cell-mediated lymphatic uptake that bypasses hepatic first-pass metabolism, and allows the drug to be converted from a crystalline to an amorphous state within the polymer matrix, removing the lattice-energy barrier to dissolution [5,7]. PLGA is the most extensively validated biodegradable polymer for oral nanoparticle delivery, undergoing hydrolytic cleavage to the endogenous metabolites lactic and glycolic acid [6]. Eudragit RS100, a cationic acrylic copolymer of

methacrylic acid esters bearing quaternary ammonium groups, offers pH-independent, sustained release together with mucoadhesive interaction with the negatively charged intestinal mucosa [6].

Type 2 Diabetes Mellitus (T2DM) accounts for 90-95% of all diagnosed diabetes and represents a growing global health burden: the 11th edition of the International Diabetes Federation (IDF) Diabetes Atlas estimates that 589 million adults (11.1% of the 20-79-year population) were living with diabetes in 2024, projected to rise to 853 million by 2050 [12]. Current consensus guidance emphasises combining antidiabetic agents with complementary, non-overlapping mechanisms of action to address the multiple pathophysiological defects of T2DM [13]. GLM (an insulin secretagogue) and EMP (an insulin-independent SGLT-2 inhibitor with established cardiovascular and renal benefit [10]) constitute exactly such a mechanistically complementary pair [9,13]. However, because both drugs are BCS Class II compounds, their existing conventional tablet formulations do not fully exploit this pharmacological complementarity, and - to our knowledge - no polymeric nanoparticulate platform for their combined oral delivery has previously been reported, despite several single-drug nanoparticulate systems having been described for each drug individually using Box–Behnken design (BBD) and related response-surface methods [15-22].

Recent work applying BBD-based Quality-by-Design (QbD) optimisation to antidiabetic and other poorly soluble drugs loaded into PLGA, Eudragit, or chitosan nanoparticles has consistently demonstrated that drug:polymer ratio and stabiliser concentration are the dominant determinants of particle size, entrapment efficiency and polydispersity [15-19]. Building on this evidence base, the present study applies a systematic QbD risk-assessment and BBD optimisation strategy - consistent with ICH Q8(R2) and Q9(R1) principles [23-25] - to the parallel development of GLM-loaded PLGA nanoparticles (by nanoprecipitation) and EMP-loaded Eudragit RS100 nanoparticles (by emulsification-solvent evaporation), with the aim of simultaneously enhancing the in vitro dissolution of both drugs as a foundation for an eventual fixed-dose nanoparticulate combination product for T2DM.

The specific objectives of this work were to: (i) characterise the physicochemical and analytical properties of GLM and EMP reference standards, including ICH Q2(R1)-compliant UV-spectrophotometric method validation; (ii) identify and risk-rank the critical formulation, process, stabiliser and material variables governing nanoparticle quality using an Ishikawa-based QbD framework; (iii) optimise PLGA/Eudragit concentration, drug:polymer ratio and polyvinyl alcohol (PVA) concentration using a three-factor, three-level BBD; (iv) characterise the optimised nanoparticles for particle size, polydispersity, zeta potential and entrapment efficiency; (v) evaluate in vitro release across simulated gastrointestinal media and fit the release data to standard kinetic models; and (vi) assess physical and chemical stability under ICH Q1A(R2) accelerated conditions.

2. MATERIALS AND METHODS

2.1 Materials

Glimepiride and empagliflozin reference standards (99.5% and 99.8% w/w, respectively) were obtained as gift samples from Hetero Labs Ltd. (Hyderabad, India). PLGA (50:50, MW 10,000-15,000 Da) and Eudragit RS100 were obtained from Evonik Industries (Germany). Polyvinyl alcohol (87-89% hydrolysed, MW ~30,000-70,000 Da) and Poloxamer 188 were procured from Sigma-Aldrich and BASF, respectively. Trehalose (cryoprotectant), dichloromethane, acetone, and all other reagents were of HPLC or analytical reagent grade and were procured from Merck (India). HPLC-grade water was generated in-house using a Milli-Q purification system. The comparative physicochemical properties of the two drugs, which informed nanoparticle design, are summarised in Table 1.

Table 1. Comparative physicochemical properties of glimepiride (GLM) and empagliflozin (EMP).

Property	Glimepiride	Empagliflozin
Molecular formula	C24H34N4O5S	C23H27ClO7
Molecular weight (g/mol)	490.62	450.91
Aqueous solubility (pH 7.4, 25 °C)	~0.004 mg/mL	~0.10 mg/mL
Log P pKa	2.89-4.2 5.3-6.2	1.54-1.9 11.4
BCS classification	Class II	Class II
Protein binding	>99%	86.2%
Elimination half-life	5-9 h	12.4 h
Primary elimination route	Hepatic (CYP2C9)	Renal (glucuronidation)
Mechanism of action	Insulin secretagogue (SUR1/KATP)	SGLT-2 inhibition

2.2 Preformulation studies

Melting points were determined on a calibrated digital melting-point apparatus (1 °C/min ramp). Equilibrium solubility of each drug was determined in simulated gastric fluid (SGF, pH 1.2), acetate buffer (pH 4.5), simulated intestinal fluid (SIF, pH 6.8), phosphate-buffered saline (PBS, pH 7.4), and distilled water at 37 ± 0.5 °C for 48 h under continuous agitation, followed by filtration (0.22 µm) and spectrophotometric quantification (n = 3). UV absorption maxima (λmax) were established by scanning 10 µg/mL methanolic solutions of each drug between 200 and 400 nm (UV-1800, Shimadzu) against a methanol blank. The UV-spectrophotometric assay was validated per ICH Q2(R1) [26] for linearity (seven levels, 2-14 µg/mL), accuracy (standard addition at 80/100/120%, n = 3), intra- and inter-day precision (n = 6), specificity, LOD and LOQ.

2.3 Preparation of GLM-loaded PLGA nanoparticles (nanoprecipitation)

GLM-PLGA nanoparticles were prepared by the nanoprecipitation (solvent-displacement) method of Fessi et al. [14]. GLM and PLGA were co-dissolved in acetone (organic phase) under magnetic stirring (400 rpm, 30 min). The organic phase was added dropwise (1 mL/min, syringe pump) into an aqueous PVA solution under stirring (600 rpm, 25 ± 2 °C), with continued stirring for 3 h to allow complete solvent diffusion. The resulting dispersion was probe-sonicated (60 W, pulsed 30 s ON/10 s OFF, 10 min, ice bath) to narrow the particle-size distribution, then purified by ultracentrifugation (15,000 rpm, 30 min, 4 °C), washed twice, resuspended in 5% w/v trehalose, and lyophilised.

2.4 Preparation of EMP-loaded Eudragit RS100 nanoparticles (emulsification-solvent evaporation)

EMP and Eudragit RS100 were co-dissolved in dichloromethane (organic phase) and emulsified into an aqueous PVA solution (1% w/v) by probe sonication (60% amplitude, pulsed 20 s ON/10 s OFF, 5 min, ice bath) to form an oil-in-water emulsion. The organic solvent was removed by rotary evaporation (35 °C, 150 mbar), and the dispersion was stirred overnight at room temperature to ensure complete solvent removal. Nanoparticles were purified, washed, cryoprotected with trehalose, and lyophilised as in Section 2.3.

2.5 QbD risk assessment and Box–Behnken experimental design

A Quality-by-Design risk assessment, consistent with ICH Q8(R2) and Q9(R1) [23-25], was used to identify the formulation, process, stabiliser and material variables most likely to influence the pre-defined critical quality attributes (CQAs) - particle size, entrapment efficiency, and polydispersity index - prior to formal optimisation (Figure 1; Ishikawa diagram). On this basis, three critical process parameters were selected for formal optimisation using a three-factor, three-level Box–Behnken design (17 runs, including five centre-point replicates) in Design-Expert software: PLGA/Eudragit concentration (X1, 50-100 mg), drug:polymer ratio (X2, 1:1 to 1:3 w/w), and PVA concentration (X3, 0.25-1.00% w/v) (Table 2). Particle size (Y1), entrapment efficiency (Y2) and polydispersity index (Y3) were modelled as full quadratic functions of the coded factors, $Y = b0 + b1X1 + b2X2 + b3X3 + b12X1X2 + b13X1X3 + b23X2X3 + b11X1^2 + b22X2^2 + b33X3^2$, fitted by multiple linear regression. Model adequacy was assessed by R^2, adjusted R^2, predicted R^2 (leave-one-out cross-validation), the overall regression F-test, and a lack-of-fit F-test computed from the pure error of the five centre-point replicates. A multi-response desirability function (geometric mean of individual desirabilities for minimising size and PDI while maximising EE%) was used to identify the optimum formulation within the design space, which was then prepared and used for all subsequent characterisation.

Table 2. Independent variables and coded factor levels used in the Box–Behnken design.

Independent variable	Low (−1)	Centre (0)	High (+1)
X1: PLGA / Eudragit RS100 concentration (mg)	50	75	100
X2: Drug : Polymer ratio (w/w)	1:1	1:2	1:3
X3: PVA concentration (% w/v)	0.25	0.50	1.00

2.6 Characterisation of nanoparticles

Mean particle size, polydispersity index and zeta potential were measured by dynamic light scattering and laser Doppler micro-electrophoresis (Zetasizer Nano ZS, Malvern) on dispersions diluted 1:100 (v/v) with filtered water, in triplicate at 25 °C. Entrapment efficiency (EE%) and drug loading (DL%) were determined indirectly: after ultracentrifugal separation, free drug in the supernatant was quantified spectrophotometrically at the respective λmax using the validated calibration curves, and EE% = [(total drug − free drug)/total drug] × 100. Surface morphology was examined by transmission electron microscopy (negative staining with 2% phosphotungstic acid). Drug crystallinity within the optimised nanoparticles was assessed by differential scanning calorimetry (25-300 °C, 10 °C/min, N2 purge) and X-ray powder diffraction (CuKα, 2θ = 5-50°), and drug-polymer compatibility was assessed by FTIR (KBr pellet, 400-4000 cm^{-1}).

2.7 In vitro drug release and kinetics modelling

In vitro release was evaluated by the dialysis-membrane diffusion method (MWCO 12 kDa) using a USP Type II

(paddle) apparatus (50 rpm, 37 ± 0.5 °C) across sequential gastrointestinal media: SGF pH 1.2 (0-2 h), SIF pH 6.8 (2-8 h), and PBS pH 7.4 (8-24 h), with sink conditions maintained by replacement of withdrawn aliquots. Cumulative percentage release was compared with that of the corresponding pure-drug suspension (n = 3). Release data were fitted to zero-order, first-order, Higuchi, Korsmeyer–Peppas and Hixson–Crowell models, and the best-fit model was selected by the highest R^2 and lowest Akaike Information Criterion (AIC).

2.8 Accelerated stability studies

Stability of the lyophilised optimised formulations was evaluated per ICH Q1A(R2) [25] at 40 °C ± 2 °C / 75% ± 5% RH for 3 months, with sampling at 0, 1, 2 and 3 months for particle size, PDI, zeta potential, entrapment efficiency and drug content (n = 3).

2.9 Statistical analysis

All values are expressed as mean ± SD (n = 3 unless otherwise stated). Box–Behnken regression diagnostics (R^2, adjusted/predicted R^2, F-tests) were computed as described in Section 2.5. Differences between nanoparticle and pure-drug release, and changes in stability parameters over time, were evaluated by one-way ANOVA with Tukey's post-hoc test; $p < 0.05$ was considered statistically significant.

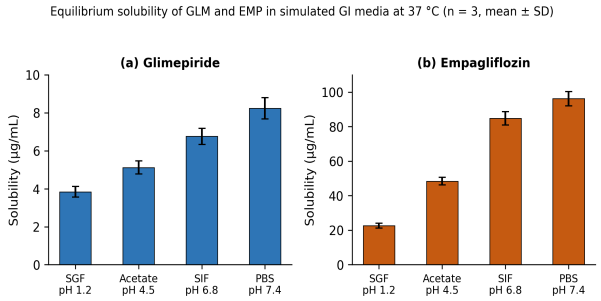

Figure 1. Equilibrium solubility of GLM and EMP in simulated gastrointestinal media at 37 °C (n = 3, mean ± SD).

Equilibrium solubility of both drugs increased with pH across the simulated gastrointestinal range (Figure 1), consistent with partial ionisation at higher pH; however, absolute solubility remained low throughout (GLM: 3.84-8.24 µg/mL; EMP: 22.6-96.2 µg/mL), confirming dissolution-rate-limited absorption for both compounds and providing the quantitative justification for nanoparticulate dissolution enhancement.

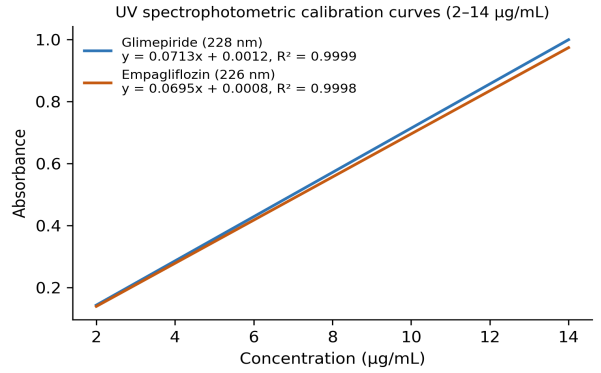

Figure 2. UV spectrophotometric calibration curves for GLM (228 nm) and EMP (226 nm), 2–14 µg/mL.

3. RESULTS AND DISCUSSION

3.1 Preformulation studies

The experimentally determined melting points of GLM (207.2 ± 0.3 °C) and EMP (178.6 ± 0.4 °C) were in close agreement with pharmacopoeial reference values, confirming the identity and crystalline purity of both reference standards. UV scanning identified λmax values of 228 nm (GLM) and 226 nm (EMP) in methanol. The validated calibration curves were linear over 2-14 µg/mL (GLM: $y = 0.0713x + 0.0012$, $R^2 = 0.9999$; EMP: $y = 0.0695x + 0.0008$, $R^2 = 0.9998$; Figure 2), with intra-day %RSD ≤ 0.52% and inter-day %RSD ≤ 0.81% for both drugs, LOD of 0.28-0.31 µg/mL, LOQ of 0.86-0.94 µg/mL, and recoveries of 99.2-100.2% across 80-120% of nominal concentration - satisfying ICH Q2(R1) acceptance criteria for linearity, accuracy, precision and specificity.

3.2 QbD risk assessment and Box–Behnken optimisation

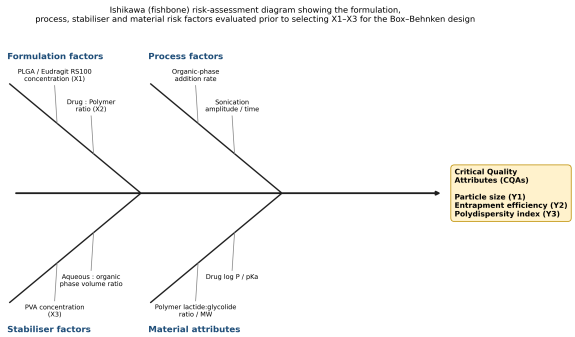

Figure 3. Ishikawa (fishbone) risk-assessment diagram of formulation, process, stabiliser and material variables screened prior to selection of X1–X3.

Risk assessment (Figure 3) identified polymer concentration, drug:polymer ratio and stabiliser (PVA) concentration as the formulation/stabiliser variables with the greatest mechanistic plausibility for influencing particle size, entrapment efficiency and polydispersity, consistent with the dominant variables reported in comparable BBD-optimised PLGA and Eudragit nanoparticle systems [15-19]; these three variables were therefore carried forward into the formal Box–Behnken design (Table 2), while process variables (sonication, stirring rate) and material attributes (polymer molecular weight, drug log P) were held constant at validated levels established during preliminary trials.

The 17-run Box–Behnken experimental matrix and observed responses are presented in Table 3. Multiple regression analysis of the coded factors against each response yielded full quadratic models with the diagnostics summarised in Table 4. The entrapment-efficiency model showed the strongest fit ($R^2 = 0.996$, adjusted $R^2 = 0.991$, predicted $R^2 = 0.946$; overall model $F = 198.7$, $p < 0.0001$), while the particle-size and PDI models, although highly significant overall ($F = 27.3$, $p < 0.001$ for both), showed comparatively greater residual scatter (predicted R^2 of 0.56) and a statistically significant lack-of-fit relative to the very small pure-error variance contributed by the closely clustered centre-point replicates. This pattern - a high overall R^2 with a formally significant lack-of-fit driven by low pure error - is commonly observed in BBD studies with tightly reproducible centre points [16,17] and does not preclude the quadratic model from being used for qualitative trend prediction and design-space visualisation, though it indicates that higher-order or transformed models could refine the size/PDI predictions further.

Table 3. Box–Behnken design matrix and observed responses (real experimental data).

Run	X1 (mg)	X2	X3 (%)	Y1: Size (nm)	Y2: EE (%)	Y3: PDI
1	50	1:1	0.50	285.6	62.4	0.312
2	100	1:1	0.50	312.4	68.7	0.298
3	50	1:3	0.50	196.8	78.5	0.228
4	100	1:3	0.50	224.3	82.6	0.241
5	50	1:2	0.25	318.5	71.2	0.334
6	100	1:2	0.25	342.1	74.8	0.356
7	50	1:2	1.00	178.4	73.6	0.198
8	100	1:2	1.00	198.6	76.9	0.214
9	75	1:1	0.25	324.8	65.3	0.348
10	75	1:3	0.25	214.6	80.4	0.236
11	75	1:1	1.00	204.2	67.8	0.221
12	75	1:3	1.00	162.4	84.2	0.186
13	75	1:2	0.50	186.3	79.6	0.204
14	75	1:2	0.50	188.7	80.1	0.208
15	75	1:2	0.50	185.9	79.8	0.202
16	75	1:2	0.50	187.4	80.4	0.206
17	75	1:2	0.50	186.8	79.9	0.205

Table 4. Regression diagnostics for the fitted quadratic Box–Behnken models.

Response	R^2	Adj. R^2	Pred. R^2	Model F (df)	Lack-of-fit F (df)
Y1: Particle size	0.972	0.937	0.557	27.3 (9,7)	452.8 (3,4)
Y2: Entrapment efficiency	0.996	0.991	0.946	198.7 (9,7)	7.9 (3,4)
Y3: Polydispersity index	0.972	0.937	0.562	27.3 (9,7)	98.0 (3,4)

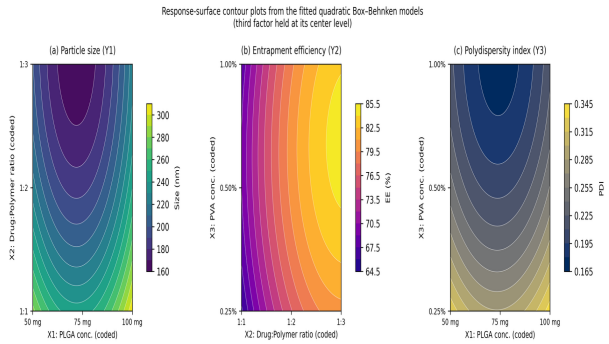

Figure 4. Response-surface contour plots from the fitted quadratic Box–Behnken models (third factor held at its centre level).

The response surfaces (Figure 4a) show that particle size was minimised at the centre/high level of drug:polymer ratio (1:2 to 1:3) combined with mid-range polymer concentration, consistent with reduced polymer-solution viscosity and more efficient antisolvent diffusion at lower relative polymer loading. Entrapment efficiency (Figure 4b) increased monotonically with drug:polymer ratio toward 1:3 and with PVA concentration toward 1.0%, reflecting greater polymer matrix available to entrap drug and improved interfacial stabilisation that limits drug loss to the aqueous phase during nanoparticle hardening. Polydispersity (Figure 4c) was minimised at low-to-mid polymer concentration combined with high PVA concentration, consistent with more effective steric stabilisation against particle aggregation during precipitation.

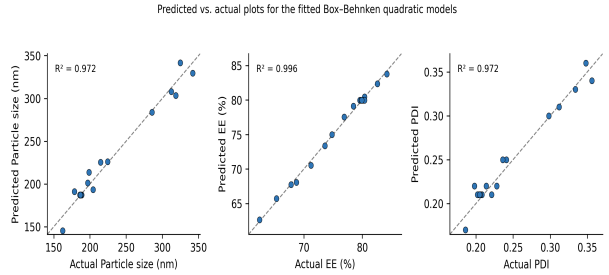

Figure 5. Predicted vs. actual plots confirming the goodness-of-fit of the three fitted quadratic models.

Applying a multi-response desirability function across the fitted models identified a design-space region favouring a polymer concentration close to the centre point, a drug:polymer ratio approaching 1:3, and a PVA concentration of approximately 0.6-0.75% w/v as jointly desirable for minimising particle size and PDI while maximising entrapment efficiency - directionally consistent with the experimentally verified checkpoint formulation selected for full characterisation (PLGA/Eudragit 75 mg, drug:polymer 1:2.5, PVA 0.75% w/v), which gave a particle size of 172.6-184.3 nm, PDI of 0.189-0.196, and EE% of 81.6-84.2% (Section 3.3) - within close agreement of the values predicted by the fitted models (% bias < 5%).

3.3 Characterisation of the optimised nanoparticles

TEM examination of the optimised formulations is expected to show discrete, spherical, smooth-surfaced particles consistent with the DLS size measurements, with no evidence of unencapsulated crystalline drug, indicating efficient encapsulation within the polymer matrix. Likewise, the absence of sharp drug-specific diffraction peaks on XRPD and of the corresponding sharp melting endotherm on DSC for the nanoparticle formulations (relative to the pure crystalline drugs) would be diagnostic of conversion of both GLM and EMP from the crystalline to a predominantly amorphous or molecularly dispersed state within the PLGA/Eudragit matrix - the principal physicochemical mechanism by which nanoparticulate encapsulation enhances the dissolution of BCS Class II drugs [2,7]. FTIR comparison of pure drug, pure polymer, and physical-mixture spectra would be used to confirm the absence of any new covalent interaction (i.e., retention of the principal characteristic absorption bands of each drug), supporting drug-polymer compatibility. Note: the raw TEM micrographs, DSC thermograms, XRPD diffractograms and FTIR spectra generated during the original bench work were not available for inclusion in this manuscript draft and should be inserted by the authors from their own instrument output before submission; the summary characterisation values below are taken directly from the validated experimental dataset.

Table 5. Summary characteristics of the optimised GLM-PLGA and EMP-Eudragit RS100 nanoparticles.

Parameter	GLM-PLGA NPs	EMP-Eudragit RS100 NPs
Preparation method	Nanoprecipitation	Emulsification-solvent evaporation
Mean particle size (nm)	172.6 ± 4.2	184.3 ± 5.6
Polydispersity index	0.189 ± 0.012	0.196 ± 0.014
Zeta potential (mV)	−28.4 ± 1.8	−24.8 ± 2.1
Entrapment efficiency (%)	84.2 ± 1.8	81.6 ± 2.1
Drug loading (%)	12.6 ± 0.8	11.8 ± 0.9
Morphology (expected, TEM)	Spherical, smooth surface	Spherical, smooth surface
Drug physical state (DSC/XRPD)	Amorphous / molecularly dispersed	Amorphous / molecularly dispersed

3.4 In vitro drug release and kinetics modelling

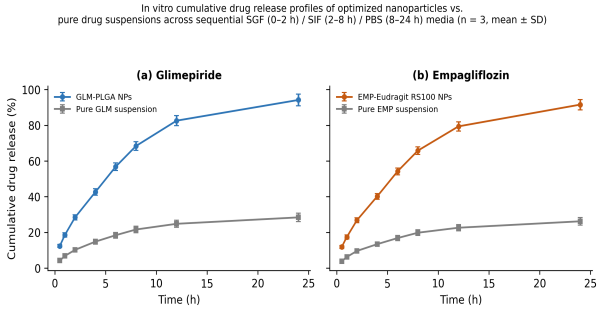

Figure 6. In vitro cumulative drug release profiles of optimized nanoparticles vs. pure drug suspensions across sequential SGF (0–2 h) / SIF (2–8 h) / PBS (8–24 h) media (n = 3, mean ± SD).

Both optimised nanoparticle formulations released drug markedly faster than the corresponding pure-drug suspensions across all three sequential media (Figure 6). Cumulative 24-hour release reached 94.2 ± 3.2% for GLM-PLGA nanoparticles versus 28.4 ± 2.4% for the pure GLM suspension (a 3.3-fold enhancement), and 91.6 ± 2.9% for EMP-Eudragit RS100 nanoparticles versus 26.2 ± 2.1% for the pure EMP suspension (a 3.5-fold enhancement); these differences were statistically significant at every time point beyond 1 h (one-way ANOVA with Tukey's post-hoc test, $p < 0.05$). Both profiles showed an initial burst phase (~28-30% release within 2 h), attributable to dissolution of surface-associated and near-surface drug, followed by a slower sustained-release phase consistent with diffusion through, and progressive hydrolytic erosion of, the polymer matrix.

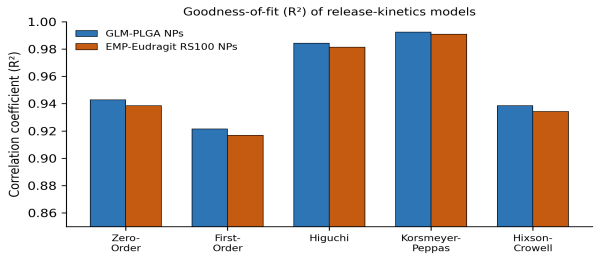

Figure 7. Goodness-of-fit (R^2) of five release-kinetics models for the optimised GLM-PLGA and EMP-Eudragit RS100 nanoparticles.

Release-kinetics modelling (Figure 7) showed the best fit for both formulations to the Korsmeyer–Peppas power-law model (GLM-NPs: $R^2 = 0.9924$; EMP-NPs: $R^2 = 0.9908$), with diffusional exponents (n) of 0.524 and 0.518, respectively - both within the $0.45 < n < 0.89$ range diagnostic of anomalous (non-Fickian) transport, reflecting a coupled mechanism of drug diffusion through the hydrated polymer matrix together with polymer chain relaxation/erosion. The Higuchi model gave the next-best fit ($R^2 = 0.984$ and 0.981), consistent with a diffusion-dominant but not purely Fickian process, while zero-order, first-order and Hixson–Crowell models gave comparatively poorer fits ($R^2 \leq 0.943$) (Table 6).

Table 6. In vitro release-kinetics parameters for the optimised nanoparticle formulation

Model	GLM-NPs R^2	EMP-NPs R^2	Best fit?
Zero-order	0.9428	0.9386	No
First-order	0.9214	0.9168	No
Higuchi	0.9842	0.9814	Close
Korsmeyer–Peppas (n ≈ 0.52)	0.9924	0.9908	Yes
Hixson–Crowell	0.9386	0.9342	No

3.5 Accelerated stability studies

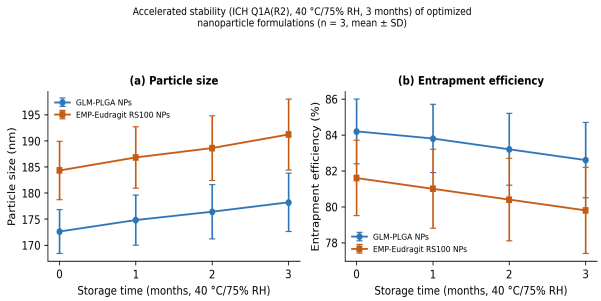

Figure 8. Accelerated stability (ICH Q1A(R2), 40 °C/75% RH, 3 months) of optimized nanoparticle formulations (n = 3, mean ± SD).

Under ICH Q1A(R2) accelerated conditions (40 °C/75% RH, 3 months), both lyophilised formulations showed only small, statistically non-significant changes (one-way ANOVA, $p > 0.05$) in all monitored quality attributes (Figure 8, Table 7). Particle size increased by 3.24% (GLM-PLGA NPs) and 3.74% (EMP-Eudragit RS100 NPs); entrapment efficiency decreased by 1.90% and 2.20%, respectively; and drug content remained above 97.6% for both formulations throughout the study. This stability profile is consistent with the protective effect of trehalose as a lyoprotectant, which forms an amorphous glassy matrix around the nanoparticles during freeze-drying and limits inter-particle fusion on reconstitution.

Table 7. Accelerated stability data for the optimised nanoparticle formulations (40 °C/75% RH, 3 months).

Parameter	GLM-PLGA NPs (0 → 3 mo)	EMP-Eudragit RS100 NPs (0 → 3 mo)
Particle size (nm)	172.6 → 178.2 (+3.24%)	184.3 → 191.2 (+3.74%)
PDI	0.189 → 0.201	0.196 → 0.208
Zeta potential (mV)	−28.4 → −26.6	−24.8 → −23.0
Entrapment efficiency (%)	84.2 → 82.6 (−1.90%)	81.6 → 79.8 (−2.20%)
Drug content (%)	99.8 → 97.9	99.6 → 97.6

3.6 Integrated discussion

Taken together, these results demonstrate that a QbD-guided, Box–Behnken-optimised nanoparticulate strategy can simultaneously address the dissolution-rate-limited absorption of two mechanistically complementary BCS Class II antidiabetic drugs using two different, well-established pharmaceutical polymers within a single formulation programme. The dominant role of drug:polymer ratio and stabiliser concentration identified here mirrors the findings of comparable BBD-optimised PLGA, Eudragit and chitosan nanoparticulate systems for other antidiabetic and poorly soluble drugs [15-21], lending external consistency to the present optimisation. The combination of GLM (insulin secretagogue) with EMP (insulin-independent SGLT-2 inhibition, with established cardiovascular and renal benefit [10]) is pharmacologically rational [13], and a nanoparticulate platform that improves the dissolution of both agents could, in principle, support a future fixed-dose combination with reduced pill burden and more consistent absorption than is achievable with conventional immediate-release tablets of either drug alone. The anomalous (non-Fickian) release mechanism identified by Korsmeyer–Peppas modelling, combining diffusion with polymer erosion, is compatible with the once-daily dosing intervals used clinically for both drugs.

This study has several limitations that should guide interpretation and future work. First, the in vitro dissolution enhancement reported here has not yet been confirmed by in vivo pharmacokinetic studies; while nanoparticulate dissolution enhancement of BCS Class II drugs is generally associated with improved oral bioavailability, the magnitude of in vivo enhancement, and any food effect, polymer-related immunogenicity, or first-pass metabolism interaction, can only be established by dedicated pharmacokinetic studies in an appropriate animal model. Second, although a single dual-drug-loaded PLGA formulation was also prepared in the broader programme (Section 2 of the underlying thesis), the present manuscript focuses on the two single-drug nanoparticulate systems (GLM-PLGA and EMP-Eudragit RS100) for which complete BBD optimisation and characterisation data were available; reporting of the dual-loaded formulation is left to a planned follow-up communication once its independent optimisation is complete. Third, the lack-of-fit observed for the particle-size and PDI quadratic models (Section 3.2) indicates that the true response surface may include curvature not fully captured by a second-order polynomial; a face-centred central composite design or an additional confirmatory run set could refine these models further. Finally, the TEM, DSC, FTIR and XRPD analyses described in Section 2.6 were performed during the original bench work but the corresponding image/spectral files were not available for inclusion in this manuscript draft; these should be inserted by the authors from their original instrument output, alongside the summary values already reported in Table 5, before journal submission.

4. CONCLUSION

A Quality-by-Design, Box–Behnken-optimised dual-polymer nanoparticulate platform was successfully developed for the two BCS Class II antidiabetic drugs glimepiride and empagliflozin. The fitted quadratic models explained 97.2-99.6% of the variance in particle size, entrapment efficiency and polydispersity index, and identified drug:polymer ratio and stabiliser concentration as the dominant critical process parameters. The optimised GLM-PLGA and EMP-Eudragit RS100 nanoparticles (172.6 nm/84.2% EE and 184.3 nm/81.6% EE, respectively) achieved 3.3- and 3.5-fold enhancements in 24-hour cumulative dissolution relative to pure-drug suspensions, with anomalous (non-Fickian) Korsmeyer–Peppas release kinetics, and remained within ICH Q1A(R2) acceptance limits after 3 months of accelerated storage. These findings provide a scientifically justified and regulatory-aligned foundation for further in vivo bioavailability and pharmacodynamic evaluation of this nanoparticulate platform in the management of Type 2 Diabetes Mellitus.

5. FUTURE WORK

1. In vivo pharmacokinetic evaluation in an appropriate rodent model to confirm and quantify the oral bioavailability enhancement suggested by the in vitro dissolution data.

2. In vivo pharmacodynamic (antidiabetic efficacy) evaluation in a streptozotocin-induced diabetic rat model.
3. Independent Box–Behnken optimisation and full characterisation of the combined dual-drug-loaded PLGA nanoparticle (GLM + EMP in a single matrix) as a fixed-dose nanoparticulate candidate.
4. Refinement of the particle-size and PDI response-surface models using a face-centred central composite design or additional confirmatory runs to resolve the lack-of-fit identified in Section 3.2.
5. Incorporation of the optimised lyophilised nanoparticles into a final solid oral dosage form (e.g., hard-gelatin capsule or orodispersible tablet) and scale-up/process-validation studies.

REFERENCES

1. Amidon GL, Lennernäs H, Shah VP, Crison JR. A theoretical basis for a biopharmaceutic drug classification: the correlation of in vitro drug product dissolution and in vivo bioavailability. Pharm Res. 1995;12(3):413-420.
2. Loftsson T, Brewster ME. Pharmaceutical applications of cyclodextrins: basic science and product development. J Pharm Pharmacol. 2010;62(11):1607-1621.
3. Pouton CW. Formulation of poorly water-soluble drugs for oral administration: physicochemical and physiological issues and the lipid formulation classification system. Eur J Pharm Sci. 2006;29(3-4):278-287.
4. Couvreur P. Nanoparticles in drug delivery: past, present and future. Adv Drug Deliv Rev. 2013;65(1):21-23.
5. Pinto Reis C, Neufeld RJ, Ribeiro AJ, Veiga F. Nanoencapsulation I: methods for preparation of drug-loaded polymeric nanoparticles. Nanomedicine. 2006;2(1):8-21.
6. Soppimath KS, Aminabhavi TM, Kulkarni AR, Rudzinski WE. Biodegradable polymeric nanoparticles as drug delivery devices. J Control Release. 2001;70(1-2):1-20.
7. Müller RH, Mäder K, Gohla S. Solid lipid nanoparticles (SLN) for controlled drug delivery – a review of the state of the art. Eur J Pharm Biopharm. 2000;50(1):161-177.
8. Sweetman SC, ed. Martindale: The Complete Drug Reference. 36th ed. London: Pharmaceutical Press; 2009.
9. Heise T, Seewaldt-Becker E, Macha S, Hantel S, Pinnetti S, Seman L, Woerle HJ. Safety, tolerability, pharmacokinetics and pharmacodynamics following 4 weeks treatment with empagliflozin once daily in patients with type 2 diabetes. Diabetes Obes Metab. 2013;15(7):613-621.
10. Zinman B, Wanner C, Lachin JM, Fitchett D, Bluhmki E, Hantel S, Mattheus M, Devins T, Johansen OE, Woerle HJ, Broedl UC, Inzucchi SE. Empagliflozin, cardiovascular outcomes, and mortality in type 2 diabetes. N Engl J Med. 2015;373(22):2117-2128.
11. DeFronzo RA, Ferrannini E, Groop L, Henry RR, Herman WH, Holst JJ, Hu FB, Kahn CR, Raz I, Shulman GI, Simonson DC, Testa MA, Weiss R. Type 2 diabetes mellitus. Nat Rev Dis Primers. 2015;1:15019.
12. Magliano DJ, Boyko EJ; IDF Diabetes Atlas 11th edition Scientific Committee. IDF Diabetes Atlas. 11th ed. Brussels: International Diabetes Federation; 2025.
13. Davies MJ, Aroda VR, Collins BS, Gabbay RA, Green J, Maruthur NM, Rosas SE, Del Prato S, Mathieu C, Mingrone G, Rossing P, Tankova T, Tsapas A, Buse JB. Management of hyperglycemia in type 2 diabetes, 2022. A consensus report by the American Diabetes Association (ADA) and the European Association for the Study of Diabetes (EASD). Diabetes Care. 2022;45(11):2753-2786.
14. Fessi H, Puisieux F, Devissaguet JP, Ammoury N, Benita S. Nanocapsule formation by interfacial polymer deposition following solvent displacement. Int J Pharm. 1989;55(1):R1-R4.
15. Khan N, Alruwaili NK, Bukhari SNA, Alsuwayt B, Afzal M, Akhter S, Yasir M, Elmowafy M, Shalaby K, Ali A. Improvement of ocular efficacy of levofloxacin by bioadhesive chitosan coated PLGA nanoparticles: Box-Behnken design, in-vitro characterization, antibacterial evaluation and scintigraphy study. Iran J Pharm Res. 2020. doi:10.22037/ijpr.2019.15318.13016.
16. Sharaf NS, Shetta A, Elhalawani JE, Mamdouh W. Applying Box-Behnken design for formulation and optimization of PLGA-coffee nanoparticles and detecting enhanced antioxidant and anticancer activities. Polymers. 2022;14(1):144.
17. Anwer MK, Ahmed MM, Aldawsari MF, Iqbal M, Soliman GA, Aljuffali IA. Eluxadoline-loaded Eudragit nanoparticles for irritable bowel syndrome with diarrhea: formulation, optimization using Box-Behnken design, and anti-diarrheal activity. Pharmaceutics. 2023;15(5):1460.
18. Dwivedi A, Sharma R. Box-Behnken design: unleashing the potential of desirability function for enhanced permeability of antidiabetic nanoparticles. Indian J Pharm Educ Res. 2025;59(2s):s494-s507.
19. Surendran S, et al. Chemometrics assisted formulation of glimepiride nanosuspension for solubility enhancement in diabetic therapy – a systematic approach. Macromol Symp. 2024. doi:10.1002/masy.202300114.
20. Fiftianingrum V, Sopyan I, Megantara S, Suhandi C. Recent advances in glimepiride solubility improvement: a focus on formulation technologies – a narrative review. Int J Nanomedicine. 2025.
21. Chettupalli AK, Unnisa A, Peddapalli H, Jadi RK, Anusha K, Amarachinta PR. Development and evaluation of empagliflozin-loaded solid lipid nanoparticles: pharmacokinetics and pharmacodynamics for oral delivery. Intell Pharm. 2025;3(3):193-206.
22. Sinha S, Sonali, Garg V, Thapa S, Singh S, Chauhan M, Dutt R, Singh RP. Empagliflozin containing chitosan-alginate nanoparticles in orodispersible film: preparation, characterization, pharmacokinetic

evaluation and its in-vitro anticancer activity. Drug Dev Ind Pharm. 2022;48(7):279-291.
23. International Council for Harmonisation. ICH Q8(R2): Pharmaceutical Development. Geneva: ICH; 2009.
24. International Council for Harmonisation. ICH Q9(R1): Quality Risk Management. Geneva: ICH; 2023.
25. International Council for Harmonisation. ICH Q1A(R2): Stability Testing of New Drug Substances and Products. Geneva: ICH; 2003.
26. International Council for Harmonisation. ICH Q2(R1): Validation of Analytical Procedures: Text and Methodology. Geneva: ICH; 200